

# Bulk optical properties of healthy female breast tissue

T Durduran<sup>1</sup>, R Choe<sup>1</sup>, J P Culver<sup>1</sup>, L Zubkov<sup>1</sup>, M J Holboke<sup>1</sup>,  
J Giammarco<sup>1</sup>, B Chance<sup>2</sup> and A G Yodh<sup>1</sup>

<sup>1</sup> Department of Physics and Astronomy, University of Pennsylvania, 209 S. 33rd Street, Philadelphia, PA 19104, USA

<sup>2</sup> Department of Biochemistry and Biophysics, University of Pennsylvania, Philadelphia, PA 19104, USA

E-mail: [durduran@stwing.upenn.edu](mailto:durduran@stwing.upenn.edu)

Received 20 March 2002

Published 24 July 2002

Online at [stacks.iop.org/PMB/47/2847](http://stacks.iop.org/PMB/47/2847)

## Abstract

We have measured the bulk optical properties of healthy female breast tissues *in vivo* in the parallel plate, transmission geometry. Fifty-two volunteers were measured. Blood volume and blood oxygen saturation were derived from the optical property data using a novel method that employed *a priori* spectral information to overcome limitations associated with simple homogeneous tissue models. The measurements provide an estimate of the variation of normal breast tissue optical properties in a fairly large population. The mean blood volume was  $34 \pm 9 \mu\text{M}$  and the mean blood oxygen saturation was  $68 \pm 8\%$ . We also investigated the correlation of these optical properties with demographic factors such as body mass index (BMI) and age. We observed a weak correlation of blood volume and reduced scattering coefficient with BMI; correlation with age, however, was not evident within the statistical error of these experiments. The new information on healthy breast tissue provides insight about the potential contrasts available for diffuse optical tomography of breast tumours.

## 1. Introduction

Near-infrared (NIR) diffuse optical tomography (DOT) is emerging as a viable means for breast tumour detection and specification. This method relies on physiological factors such as blood volume (total haemoglobin concentration), blood oxygen saturation (ratio of oxy-haemoglobin to total haemoglobin concentration), water, lipid content and tissue scattering to enhance tumour specificity and sensitivity. Thus far, *in vitro* optical properties of breast have been reported (Cheong *et al* 1990, Peters *et al* 1990, Troy *et al* 1996, Bevilacqua *et al* 1997, Gayen and Alfano 1999), and pilot *in vivo* measurements of endogenous optical properties and endogenous tumour contrast

have been reported (Chance 1998, Kang *et al* 1993, Suzuki *et al* 1996, McBride *et al* 1999, Delpy and Cope 1997, Painchaud *et al* 1999, Tromberg *et al* 1997, Fishkin *et al* 1997, Cerussi *et al* 2001, 2002, Grosenick *et al* 1999, Franceschini *et al* 1997, Sickles 1984, Nioka *et al* 1994, Hoogeraad *et al* 1997, Ntziachristos *et al* 1998, 1999, 2000, Pogue *et al* 2001a, 2001b). The use of exogeneous contrast agents has also been investigated (Gurfinkel *et al* 2000, Ntziachristos *et al* 1999, 2000, Ntziachristos and Chance 2001, Weissleder *et al* 1999, Hawrysz and Sevick-Muraca 2000, Mahmood *et al* 1999, Li *et al* 1985, O'Leary *et al* 1994, Sevick-Muraca and Burch 1994, Li *et al* 1996, Boas *et al* 1993). Indocyanine green (ICG) for example, was demonstrated to enhance breast tumour contrast *in vivo* (Gurfinkel *et al* 2000, Ntziachristos *et al* 1999, 2000, Ntziachristos and Chance 2001). Similar results were obtained with optically quenched near-infrared fluorescence dyes (Weissleder *et al* 1999, Hawrysz and Sevick-Muraca 2000, Mahmood *et al* 1999), suggesting that early detection of tumours may be possible. For a recent review of developments in optical methods in breast cancer diagnostics with emphasis on fluorescent contrast agents see Hawrysz and Sevick-Muraca (2000).

Diffuse optical tomography differs from its predecessor, diaphanography (Watmough 1982, Bartrum and Crow 1984, Alveryd *et al* 1990, Cutler 1929), because it employs a rigorous mathematical model for the propagation of photons in tissues. The diffusion model enables experimenters to separate tissue scattering effects from tissue absorption effects, and thus extract more quantitative information about tissue chromophores. The diffusion model can also be adapted to ameliorate a variety of complications that arise from tissue boundary (Fantini *et al* 1996), multi-layer effects (Franceschini *et al* 1999) and the heterogeneous structure of the tissue (Cubeddu *et al* 2000a). Finally the diffusion model provides a sound mathematical basis for data inversion and tomographic image reconstruction (Arridge and Hebden 1997).

This paper is concerned with the optical properties of healthy breast tissue. Since we are ultimately interested in differentiating diseased tissue from healthy tissue, it is desirable to measure and understand the properties of healthy tissues, including their variation with time and demographics. Thus far a few investigators have probed such changes with respect to hormone levels during the menstrual cycle (Cubeddu *et al* 2000b, 2000c), menopause (Suzuki *et al* 1996, Chance 1998, Cerussi *et al* 2001), age (Chance 1998, Tromberg *et al* 1997, Cerussi *et al* 2001, 2002, Cubeddu *et al* 1999, Suzuki *et al* 1996) and body mass index (BMI) (Pogue *et al* 2001a, Suzuki *et al* 1996, Cerussi *et al* 2002). Each of these investigations has particular strengths and weaknesses.

Suzuki *et al* (1996) studied the optical properties of 30 Japanese women. They employed a time-resolved optical system in the transmission geometry for measurement, but only a single wavelength and a single source–detector pair was employed. Nevertheless, they reported strong correlation of absorption and scattering properties with age, BMI and menstrual status; no correlation was observed with respect to breast thickness and pregnancy number. Cerussi *et al* (2001) recently published observations of 28 volunteers. These experiments improved on earlier measurements by using a multi-wavelength, multi-modulation-frequency optical system; however, the device utilized a single source–detector pair at relatively small separation and thus probed primarily within 1 cm of the tissue surface. Such tissue generally contains more fat. Their experiments revealed substantial changes in the breast tissue optical properties between pre- and post-menopausal women; some correlation between age and blood volume, water content and ‘scatter power’ were found, but the most important observation was that older breast tissues had different water and lipid content. A newer study using the same instrument (Cerussi *et al* 2002), with 30 volunteers further related their findings to BMI to verify the accuracy of the extracted lipid fraction and the relationship of the ‘scatter power’ to BMI. Cubeddu *et al* (2000b, 2000c) followed the tissue optical properties at multiple wavelengths

between 610–1010 nm throughout the menstrual cycle and quantified the changes for one volunteer. They reported changes with age, which could be attributed to tissue fat content (Cubeddu *et al* 1999). Finally, Pogue *et al* (2001a, 2001b) investigated 16 normal breasts using a cylindrical DOT system geared towards imaging. They found that blood volume was correlated with body mass index (BMI), but found no other strong correlations.

In this paper we present measurements of 52 healthy volunteers using our clinical diffuse optical imager in the compressed breast geometry. Informed consent was obtained from volunteers and the measurements were carried out over 18 months at the Hospital of University of Pennsylvania under local internal review board (IRB) approval. Our instrument was a prototype geared towards diffuse optical tomography in the parallel plate transmission geometry with soft compression. We used a single modulated source centrally located on one plate, and 153 detectors on the opposite plate. Measurements were performed at three wavelengths (830 nm, 786 nm, 750 nm). The modulation frequency was 140 MHz providing the phase and amplitude of 153 diffuse photon density waves (DPDWs) in transmission. Thus our measurements were sensitive to the bulk of the breast tissue (as opposed to near-surface tissues). For data analysis we employed a new scheme that utilized *a priori* information about the expected spectral dependence of scattering and absorption in a simple, infinite slab model; this ‘physiologically constrained’ approach substantially reduced inter-parameter cross-talk in our estimates of bulk optical properties. We directly obtain chromophore concentrations and scattering parameters as a result of these fits.

The haemoglobin concentrations thus obtained were used to calculate blood volume and blood oxygen saturation. Histograms of all properties provide new estimates of the range of healthy breast properties. The combination of blood volume and blood oxygen saturation information enables us to define ranges of tumour optical properties wherein substantial endogenous contrast should arise. The properties were related to age and body mass index (BMI); the latter exhibited some correlation with blood volume and with the reduced scattering coefficient. Physiological measurement noise was also estimated by repeated measurements of the same breast and by repeated measurements at a given detector position.

## 2. Instrumentation and clinical setting

Our optical breast imager is illustrated schematically in figure 1. We employ a parallel plate, transmission geometry with soft compression. The instrument uses three wavelengths—830 nm, 786 nm and 750 nm, and employs a scanning, fibre-coupled PMT detector (R928, Hamamatsu) for detection. The system is characterized by a noise equivalent power of  $\approx 0.1 \text{ pW Hz}^{-1/2}$ , a linearity in amplitude of 1%, and a phase drift of  $0.25^\circ$  over 80 dB. We calibrated the instrument over a broad range of input powers in order to extend this range. For transmission measurements the signal variation is typically  $\approx 30 \text{ dB}$ . In clinical measurements we utilize a single source position at the centre of the scanning region. The lasers are amplitude modulated at 140 MHz to produce diffuse photon density waves (DPDWs) in the medium. The amplitude and phase of the DPDW is recovered using a homodyne IQ-demodulation scheme (Yang *et al* 1997). Figure 1 shows a sketch of the electronics.

We have characterized the instrument with extensive phantom studies (Durduran *et al* 1999a, 1999b, 2000, 2001). More recently and as a result of our experience in pilot studies on volunteers, we have constructed a more complex imaging device in the same apparatus which combines RF and CW measurements (Culver *et al* 2000, 2002).

For the *in vivo* measurements the volunteer lies in the prone position. Her breast is inserted into a small tank filled with a near-matching solution of Intralipid and India-ink mixture (see figure 1). The detector is scanned along the output plate glass surface. The source is

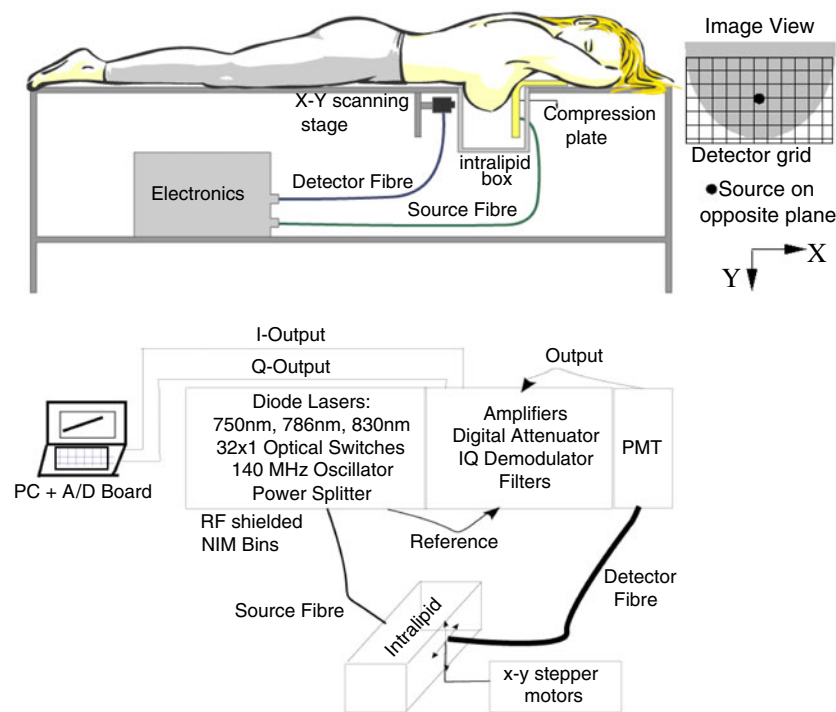


**Figure 1.** A sketch of the prototype clinical table. The volunteer lies in the prone position with her breast inserted into the tank through a large aperture on the bed. Soft compression is applied on the source plane and detector scans a 2D grid on the opposite plane. The image view shows the source detector positions as seen in the data. The lower inset shows the sketch of the system including the electronic components.

attached to the movable compression plate, which applies a gentle compression to the breast. The usual range of compression is 4.5 cm to 7 cm. It took  $\approx 15$  min to acquire data from a 9.6 cm ( $x$ ) by 4.8 cm ( $y$ ) scan region with 153 ( $17 \times 9$ ) measurement points. Feedback from volunteers was generally positive; compared to x-ray mammography, the soft-compression of the DOT instrument did not cause discomfort. We obtained two sets of data for each volunteer: (1) a measurement of the tank filled with Intralipid solution, without the breast, which allows us to normalize the instrument response for imaging purposes and to obtain an estimate of the breast tissue boundaries. (2) A measurement from the tank filled with Intralipid solution and the volunteer's breast. The Intralipid helps to reduce the detrimental effects of breast boundaries by acting as a matching medium. Measurements were repeated to assess physiological noise.

### 3. Theory and analysis

We modelled our parallel plate geometry as an infinite slab, bounded on one side by a glass window (the detector plane) and on the other by a white plate (the source plane). Previously (Durduran *et al* 1999a) we have shown that the chest wall affects the acquired data by effectively extending the diffusive medium above the tank; in practice this makes our infinite

slab approximation even better. Special care was taken during the data acquisition to centre the source and the detector grid on the breast tissue; however, occasionally some regions from outside the breast tissue were also in the field of view. In such cases we ignored grid points near the boundaries in our analyses. The solution for an infinite slab is obtained using image sources and is well known (Haskell *et al* 1994, Contini *et al* 1997, Martelli *et al* 1997).

For chromophore analysis, we employ a simple algorithm that utilizes *a priori* spectral information to reduce inter-parameter crosstalk (Durduran *et al* 2001). We outline this method below.

We decompose the absorption coefficient ( $\mu_a$ ) into contributions from different tissue chromophores, i.e.

$$\mu_a(\lambda) = \sum_i^{NC} \epsilon_i(\lambda) c_i. \quad (1)$$

Here the sum is over the different tissue chromophores and  $NC$  is the number of chromophores included in the sum.  $\epsilon_i(\lambda)$  is the wavelength-dependent extinction coefficient of the  $i$ th chromophore (obtained from the literature (Prahl 2001)<sup>3</sup>), and  $c_i$  is the concentration of the  $i$ th chromophore. The  $c_i$  are unknowns. Oxy- and deoxy-haemoglobin are the most significant chromophores in our spectral region. They can be combined to obtain blood volume (i.e. total haemoglobin concentration) and blood oxygen saturation. These quantities are important physiological tissue properties. For healthy breast tissue, the primary absorbers in our near infrared window are oxy- and deoxy-haemoglobin, lipid and water (Cerussi *et al* 2001). Because we used only a limited number of wavelengths, we introduced a relatively small, wavelength-dependent background absorption based on water and lipid signals measured by optical spectroscopy (Cerussi *et al* 2001). The water and lipid content of breast are taken to be 31% and 57%, respectively (White *et al* 1987, Woodard and White 1986, Lee *et al* 1997).

The other parameter characterizing the migration of photons through tissue is the reduced scattering coefficient ( $\mu'_s$ ). It has been shown that a simple Mie-scattering approximation is applicable to scattering from breast tissues (Cerussi *et al* 2001, Pogue *et al* 2001a, Cubeddu *et al* 1999, 2000b). Within this approximation we write  $\mu'_s$  as (Mourant *et al* 1997, Nilsson *et al* 1998)

$$\mu'_s(\lambda) = ax^b \lambda^{-b} \quad (2)$$

where  $a$ ,  $b$  are free parameters.  $a$  is proportional to the density of the scattering centres and  $b$  depends on their size.  $x = 2\pi r n_m$  where  $n_m$  is the index of refraction of the medium and  $r$  is the homogeneous sphere radius for a 'typical scatterer'. For breast tissue with a distribution of different size scatterers, we define a 'Mie-equivalent radius' ( $r = r_e$ ) as an 'average' scatterer size (Nilsson *et al* 1998), and use a simplified version of equation (2), which has been shown to be a reasonably good approximation over the wavelength range we employ, and wherein the  $x$  dependence is lumped into the coefficient  $A$ :

$$\mu'_s(\lambda) = A\lambda^{-b}. \quad (3)$$

Cerussi *et al* (2001) have found empirically that  $b$  (called the 'scatter power') is a good indicator of changes in breast tissue physiology with age. Our fitted values of the scattering parameters  $a$  and  $b$  are not very precisely obtained as a result of the limited number of wavelengths used in our study, e.g.  $b$  was measured to be  $1.27 \pm 0.82$ .

We formulate the inversion problem in terms of the variables described above assuming an infinite slab model. Traditionally  $\mu_a$  and  $\mu'_s$  are reconstructed for each wavelength separately.

<sup>3</sup> We kindly thank S J Matcher for providing the spectra for lipids.

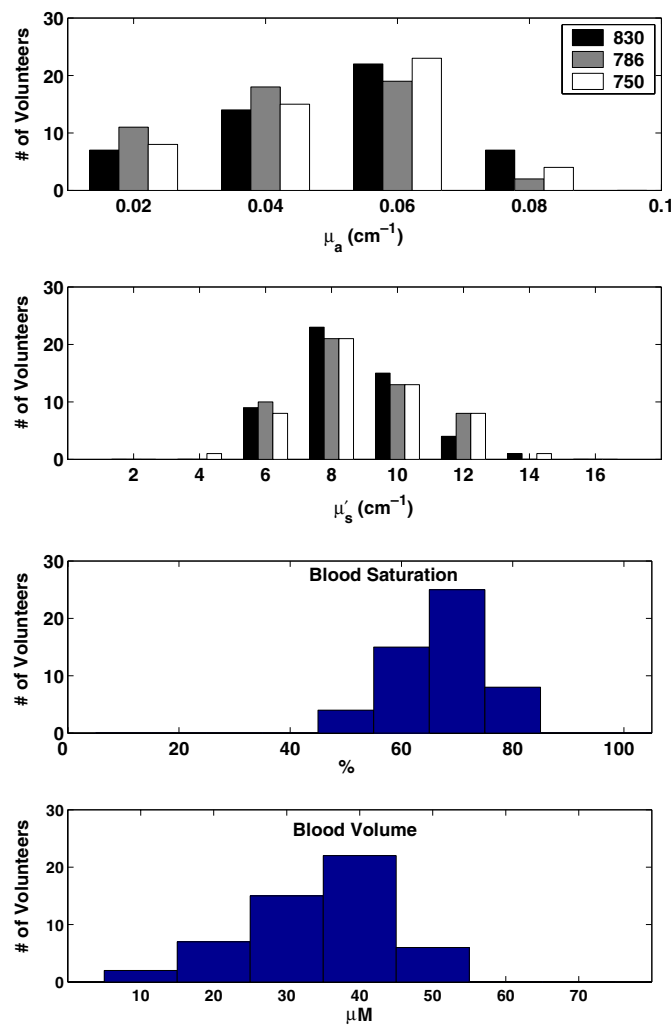


**Figure 2.** Starting from the top, shown are  $\mu_a$ ,  $\mu'_s$ , blood oxygen saturation and blood volume histograms.

However, due to model mismatch, and experimental and physiological noise, significant inter-parameter cross-talk is introduced by the standard procedure, often leading to large errors in blood volume and saturation. Instead, we directly reconstruct the concentrations ( $c_i$ ),  $A$ , and  $b$ . This procedure constrains the fitting algorithm using *a priori* spectral information. Thus we globally analyse the whole set of data, instead of analysing each wavelength independently and then combining the results. This approach substantially reduces the inter-parameter cross-talk (Durduran *et al* 2001).

In the calculation we minimize  $\chi^2 = \sum |\Phi_m - \Phi_c|^2$  where  $\Phi_m$  is the measured fluence and  $\Phi_c$  is the calculated fluence. The sum is over the source detector pairs and all wavelengths. We use the Nelder–Mead simplex (direct search) method implemented in MATLAB function ‘fminsearch’ to fit for the unknowns by minimizing  $\chi^2$ . We then calculate blood oxygen saturation and blood volume from the relevant haemoglobin concentrations.

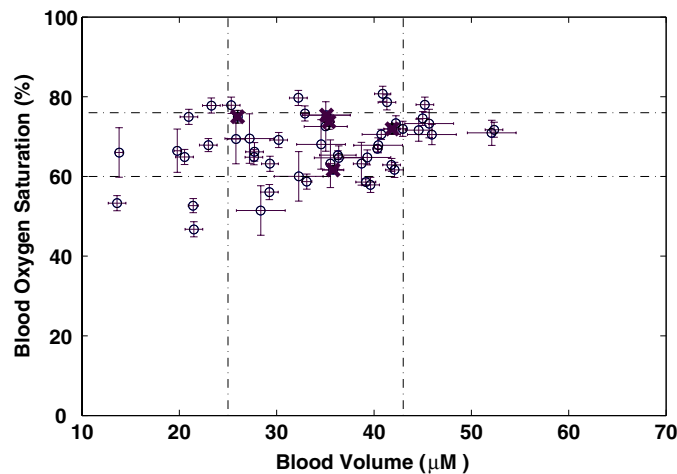


**Figure 3.** Blood oxygen saturation versus blood volume with the dashed lines indicating the ranges for normal tissue from the mean and standard deviation of the healthy breast tissue. Crosses (×) indicate menopausal volunteers.

**Table 1.** Average optical properties, physiological parameters and standard deviation from the histograms.

|                              |                   |                   |                   |
|------------------------------|-------------------|-------------------|-------------------|
| $\lambda$ (nm)               | 830               | 786               | 750               |
| $\mu_a$ (cm <sup>-1</sup> )  | $0.046 \pm 0.027$ | $0.041 \pm 0.025$ | $0.046 \pm 0.024$ |
| $\mu'_s$ (cm <sup>-1</sup> ) | $8.3 \pm 2.0$     | $8.5 \pm 2.1$     | $8.7 \pm 2.2$     |
| Blood volume (μM)            | $34 \pm 9$        |                   |                   |
| Blood oxygen saturation (%)  | $68 \pm 8$        |                   |                   |

## 4. Results and discussion

### 4.1. Optical properties of healthy breast tissue

In order to establish a range of optical and physiological properties for the healthy breast tissue we made histograms of the fitted properties. The results are summarized in figure 2. The values lie within the expected physiological range. Mean and standard deviation are shown in table 1.

Some researchers have speculated that tumours and other diseased tissue are distinguished from normal tissues by the relative value of their blood volume and blood oxygen saturation. For example, malignant tumours might be expected to have high blood volume with a low oxygen saturation since both a higher blood content and higher metabolism are necessary to achieve tumour growth in proliferating tumour tissue (Thomsen and Tatman 1998). Figure 3 shows blood oxygen saturation plotted versus blood volume for each breast (crosses (×) indicate menopausal volunteers). The dashed lines indicate the measured range of blood volume and blood oxygen saturation for normal breasts from table 1 (i.e. the mean and standard deviation). The error bars for each individual are obtained from the standard deviation of repeated measurements of the same breast. In order to employ endogeneous contrast effectively in breast DOT, tumour tissue properties should ideally lie in one of the 'other' regions defined on this plot.

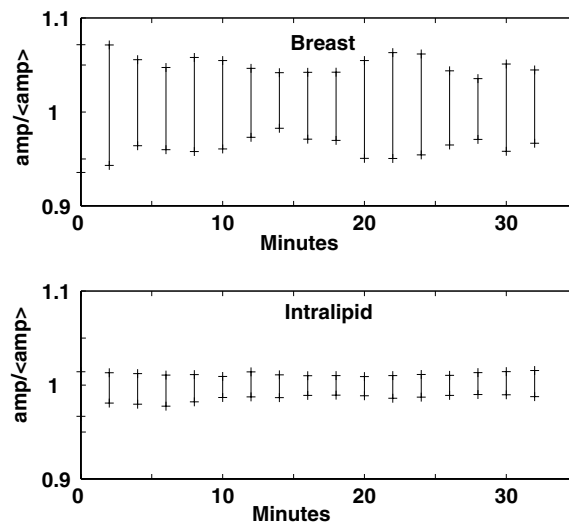


**Figure 4.** Normalized amplitude measured on breast and Intralipid sample by visiting the same 17 points every two minutes ten times.

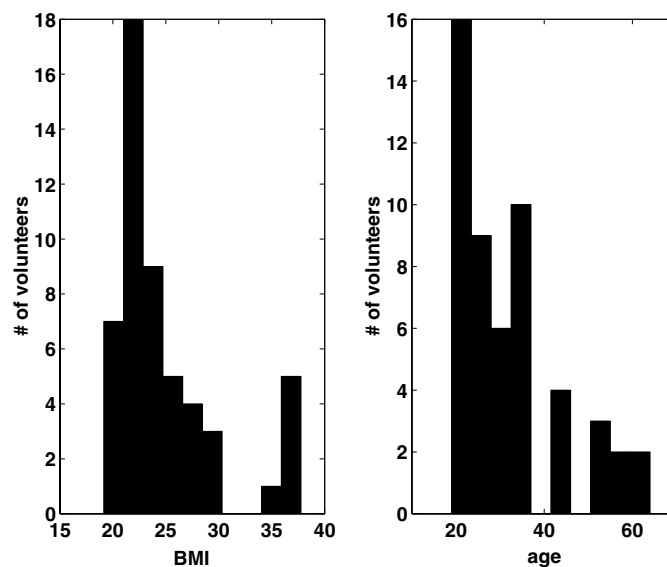


**Figure 5.** Distribution of patients in terms of their body mass index (BMI) (left) and age (right).

#### 4.2. Physiological noise

Apart from characterizable noise due to electronics, optics and positioning of the sources and detectors, there is additional noise in the measurements as a result of changes in the physiological state of the tissue during the measurements. Respiration, movement, heart beat and blood flow downstream of the hanging breast are some factors that contribute to this ‘physiological noise’.



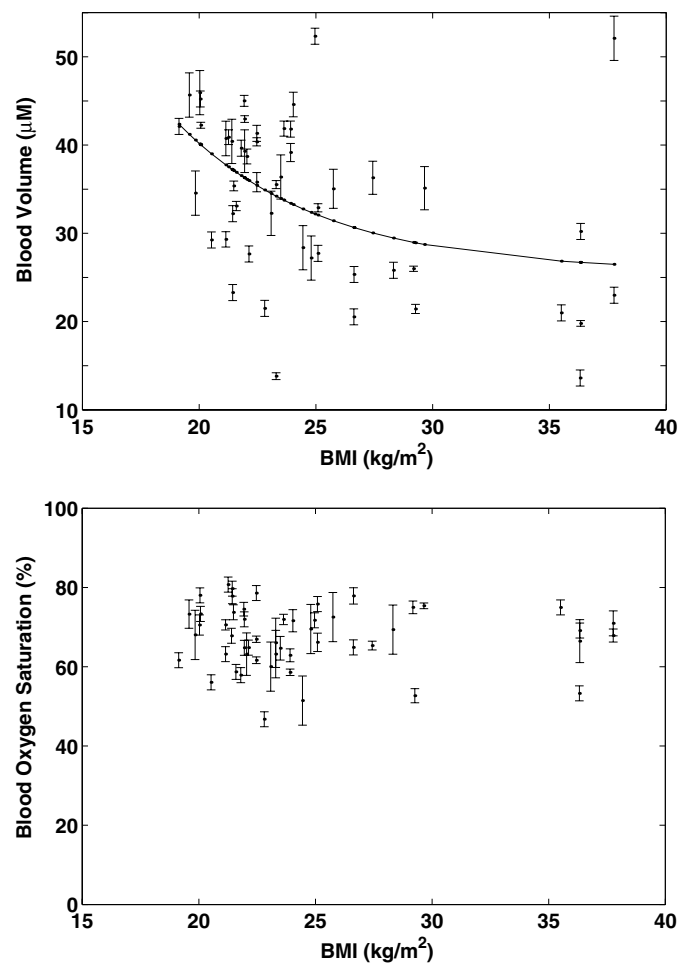


**Figure 6.** Top: blood volume versus BMI with a decaying exponential fit (correlation coefficient 0.42); bottom: blood oxygen saturation (correlation coefficient 0.03) versus BMI.

In order to estimate this effect, the scanning detector was modified to repeat each of the 17 source–detector combinations ten times every two minutes. The main results are shown in figure 4 where we plot the time series of normalized amplitude (phase is not shown) obtained from measurements on an Intralipid sample and on breast tissue. The signals from the Intralipid are stable to within 1–2%, whereas the breast tissue has dispersions of 5–10%. This provides us with an estimate of the physiological noise in our experiments.

We also performed repeated measurements of the same breast with minimal movement of the breast. By comparing repeated measurements, we find that the average standard deviation is 11% for  $\mu_a$ , 4% for  $\mu'_s$ , 4% for blood oxygen saturation and 5% for blood volume (see, for example, error bars in figure 3). These values are consistent with the variations in the amplitude and phase observed in figure 4.

#### 4.3. Demographics and optical properties

As mentioned above, it might be expected that optical properties would show a variation with demographics. We investigated the correlation of our results with two demographic quantities:

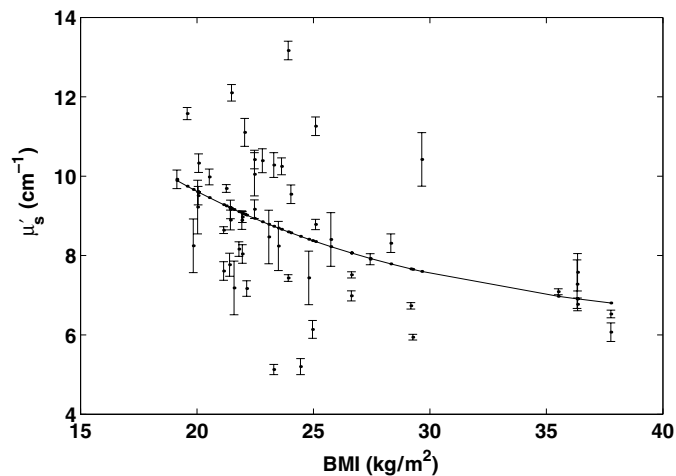


**Figure 7.**  $\mu'_s$  at 830 nm versus BMI with a decaying exponential fit. Other wavelengths show similar trends. The correlation coefficient is 0.46.

body mass index (BMI) and age, whose distributions are shown in figure 5. The mean (standard deviation) age of the volunteer population lies in the radiographically dense population and it is  $32 \pm 12$  years. The mean (standard deviation) BMI is  $25 \pm 5$ . Only five patients were menopausal and one patient was peri-menopausal. Our study was not originally aimed towards establishing correlations with demographic factors and future studies will be further optimized for looking specifically at those aspects of the problem. Specifically, we have used only three wavelengths and assumed flat water and lipid concentration in our analysis. This limits our spectral information which further limits the quality of these correlations (Cerussi *et al* 2002). Further spatial information would also be valuable in distinguishing different regions of the breast tissue. With these caveats, we now outline our findings and compare them to the results available in the literature from other studies. Pogue *et al* (2001a) used a similar system geared towards imaging and reported that blood volume had a correlation with body mass index (BMI) which relates the weight and height of an individual. They did not report strong correlation between any other quantities and BMI or age. Cerussi *et al* (2001) reported weak correlation between blood volume and scatter power ( $b$ ) with age and measured changes of lipid concentration with age and BMI (Cerussi *et al* 2002).

Our findings are shown in figure 6 for correlations with BMI. Our observed correlation of blood volume to BMI is similar to reports by Pogue *et al* (2001a). A higher BMI indicates more tissue fat content. In compositional studies, a higher fat content correlates with a lower blood content (Thomsen and Tatman 1998, Duck 1990, White *et al* 1987, Woodard and White 1986, Gertig *et al* 1999, Lee *et al* 1997). The correlation coefficient is significantly higher for blood volume than for blood oxygen saturation (0.42 versus 0.03).

We also observed a similar correlation of BMI and  $\mu'_s$  as shown in figure 7. Cerussi *et al* (Cerussi *et al* 2001, 2002) showed that the scattering power and  $\mu'_s$  change with the fat content. BMI is a measure of the tissue fat content, hence the present result is in qualitative agreement with their observations.

Figure 8 shows the correlation of the blood volume and blood oxygen saturation with age. Our results again indicate an agreement with Pogue *et al* (2001a); we do not see any

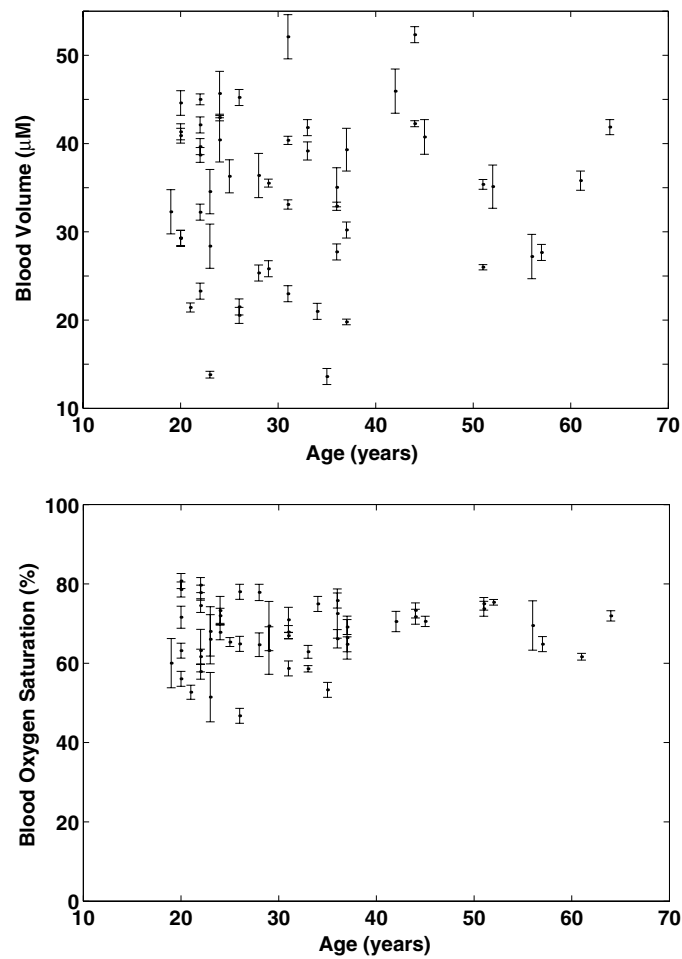


**Figure 8.** Top: blood volume versus age. The correlation coefficient is 0.0292. Bottom: blood oxygen saturation versus age. The correlation coefficient is 0.15.

clear correlations within our current signal-to-noise. As shown in figure 9 we do not see a correlation of  $\mu'_s$  with age as well.

Our study had a different sensitivity to that of Cerussi *et al* (2001, 2002) who showed that there is considerable change in breast properties with age. Their main observation is that older breast tissue has a different water and lipid content, which in turn affects the scattering and absorption properties of the tissue. We suspect their instrument was particularly sensitive to this aspect because it measured mainly the outer  $\approx 1$  cm of the tissue and had many wavelengths which allowed more accurate derivation of the wavelength dependence of the scattering. Our results, by contrast, sample a larger volume in transmission geometry. Therefore, we sample the fatty tissue as well as the nodules and vasculature extensively. There are expected changes in the breast tissue structure with age throughout the total volume, however, our study was not sensitive to those changes as it did not attempt to distinguish different regions of the breast tissue. We are not sensitive to lipid content because of our limited spectral information and because of our assumptions regarding the lipid and water content of the breast. The latter

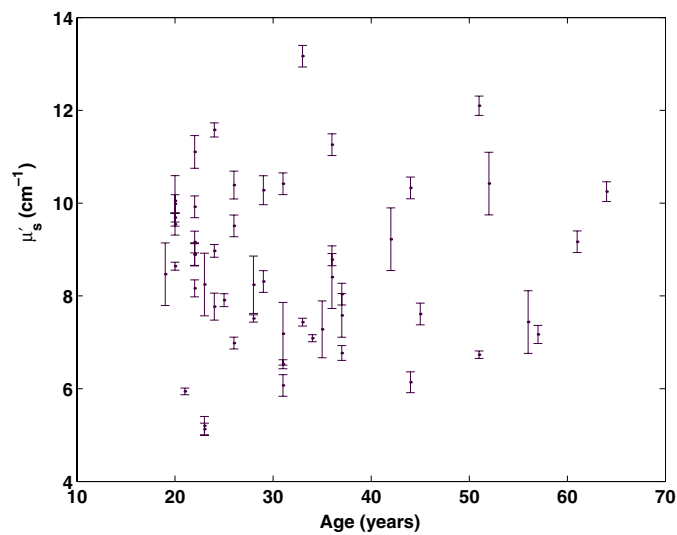


**Figure 9.**  $\mu'_s$  at 830 nm versus age. Other wavelengths show similar trends. The correlation coefficient is 0.02.

was shown to introduce errors in an analysis by Cerussi *et al* (2002). This fact, of course, points further to the need for diffuse optical imaging with extensive spectral information. Our results are important, because they establish baseline optical properties in the transmission plate geometry, and most imaging systems rely on sampling a large volume of the breast tissue. Indeed it has previously been reported that differences in acquisition geometry can induce changes in bulk properties (Cubeddu *et al* 2000b, 2000a).

## 5. Conclusion

The bulk optical properties of healthy female breast tissue were measured *in vivo* in a parallel plate, with transmission geometry geared towards diffuse optical tomography. Fifty-two volunteers with healthy breasts were measured. The analysis was done with a novel method which employs *a priori* spectral knowledge to overcome the shortcomings of simplified models of the heterogeneous breast tissue. Our results establish a range for the healthy breast properties in this geometry over a fairly large population. The blood volume was  $34 \pm 9 \mu\text{M}$  and blood oxygen saturation was  $68 \pm 8\%$  (see table 1). We investigated the correlation of optical properties with demographic properties and observe a weak correlation of blood volume and reduced scattering coefficient with body mass index.

## Acknowledgments

This work was supported by NIH 2-RO1-CA-75124-04, Army DAMD17-00-1-0408 grants. We gratefully acknowledge useful discussions with D N Pattanayak, C Cheung, X Intes, J Ripoll, B W Pogue and B J Tromberg who provided useful insights into acquisition and analysis of these datasets. We also thank L Pfaff, C Cowan and K Thrush for their help in clinical measurements and, Y K Choe for his help in illustrations.

## References

- Alveryd A, Andersson I and Aspegren K 1990 Light scanning versus mammography for the detection of breast cancer in screening and clinical practice: a Swedish multicenter study *Cancer* **65** 1671–77
- Arridge S R and Hebden J C 1997 Optical imaging in medicine: II. Modelling and reconstruction *Phys. Med. Biol.* **42** 841–54
- Bartrum R J and Crow H C 1984 Transillumination light scanning to diagnose breast cancer: a feasibility study *Am. J. Roentgen.* **142** 409–14
- Bevilacqua F, Marquet P, Coquoz O and Depeursinge C 1997 Role of tissue structure in photon migration through breast tissues *Appl. Opt.* **36** 44–48
- Boas D A, O'Leary M A, Chance B and Yodh A G 1993 Scattering and wavelength transduction of diffuse photon density waves *Phys. Rev. E* **47** 2999–3002
- Cerussi A E, Berger A J, Bevilacqua F, Shah N, Jakubowski D, Butler J, Holcombe R F and Tromberg B J 2001 Sources of absorption and scattering contrast for near-infrared optical mammography *Acad. Radiology* **8** 211–18
- Cerussi A E, Jakubowski D, Shah N, Bevilacqua F, Lanning R, Berger A J, Hsiang D, Butler J, Holcombe R F and Tromberg B J 2002 Spectroscopy enhances the information content of optical mammography *J. Biomed. Opt.* **7** 60–71
- Chance B 1998 Near-infrared images using continuous, phase-modulated, and pulsed light with quantitation of blood and blood oxygenation *Adv. Opt. Biop. and Opt. Mammography, Ann. of New York Acad. of Sci.* **838** 19–45
- Cheong W F, Prael S A and Welch A J 1990 A review of the optical properties of biological tissues *IEEE J. Quantum Electron.* **26** 2166–85
- Contini D, Martelli F and Zaccanti G 1997 Photon migration through a turbid slab described by a model based on diffusion approximation: I. Theory *Appl. Opt.* **36** 4587–99
- Cubeddu R, D'Andrea C, Pifferi A, Taroni P, Torricelli A and Valentini G 2000a Spatial changes in the absorption spectrum of the female breast *Optical Society of America Biomedical Topicals Meeting (Miami, FL)* pp 419–21
- Cubeddu R, D'Andrea C, Pifferi A, Taroni P, Torricelli A and Valentini G 2000b Effects of the menstrual cycle on the red and near-infrared optical properties of the human breast *Photochem. Photobiol.* **72–73** 383–91
- Cubeddu R, D'Andrea C, Pifferi A, Taroni P, Torricelli A and Valentini G 2000c Effects of the menstrual cycle on the red and near-infrared optical properties of the human breast *Optical Society of America Biomedical Topicals Meeting (Miami, FL)* pp 323–25
- Cubeddu R, Pifferi A, Taroni P, Torricelli A and Valentini G 1999 Noninvasive absorption and scattering spectroscopy of bulk diffusive media: an application to the optical characterization of human breast *Appl. Phys. Lett.* **74–76** 874–6
- Culver J P, Choe R, Holboke M J, Zubkov L, Durduran T, Slemple A, Ntziachristos V, Chance B and Yodh A G 2002 Three-dimensional diffuse optical tomography in the parallel plane transmission geometry: evaluation of a hybrid frequency domain/continuous wave clinical system for breast imaging *Med. Phys.* at press
- Culver J P, Ntziachristos V, Zubkov L, Durduran T, Pattanayak D N and Yodh A G 2000 Data set size and image quality in diffuse optical mammography: evaluation of a clinical proto type *Optical Society of America Biomedical Topicals Meeting (Miami, FL)* pp 392–94
- Cutler M 1929 Transillumination as an aid in the diagnosis of breast lesions *Surgery, Gynecol. Obstet.* **48** 721
- Delpy D T and Cope M 1997 Quantification in tissue near-infrared spectroscopy *Philos. Trans. R. Soc. Lond. B: Biol. Sci.* **352** 649–59
- Duck F A 1990 *Physical Properties of Tissue* (New York: Academic) pp 320–28
- Durduran T, Culver J P, Zubkov L, Choe R, Holboke M J, Chance B and Yodh A G 2001a Bulk optical properties of normal female breasts measured with a frequency domain clinical imager *Photonics West 2001, SPIE* vol 4250–65
- Durduran T, Culver J P, Zubkov L, Choe R, Holboke M, Pattanayak D N, Chance B and Yodh A G 1999a Bulk optical properties of normal breasts and tissue phantoms obtained with clinical optical imager *Proc. Inter-Institute Workshop on In Vivo Optical Imaging at the NIH (Bethesda, MD)* ed A H Gandjbakhche, pp 130–35
- Durduran T, Culver J P, Zubkov L, Choe R, Holboke M J, Pattanayak D N, Chance B and Yodh A G 2000 Bulk optical properties of normal breasts and tissue phantoms obtained with clinical optical imager *Optical Society of America Biomedical Topicals Meeting (Miami, FL)* pp 386–8
- Durduran T, Culver J P, Zubkov L, Holboke M J, Choe R, Li X D, Chance B, Pattanayak D N and Yodh A G 1999b Diffraction tomography in diffuse optical imaging; filters and noise *Photonics West 1999, SPIE* vol 3597–101 (San Jose, CA: SPIE)

- Durduran T, Giammarco J, Culver J P, Choe R, Zubkov L, Holboke M J, Yodh A G and Chance B 2001b Explicit inclusion of chromophore absorption and scattering spectra for diffuse optical imaging and spectroscopy *Photonics West 2001, SPIE* vol 4250–85
- Fantini S, Franceschini M A, Gaida G, Gratton E, Jess H and Mantulin W W 1996 Frequency-domain optical mammography: edge effect corrections *Med. Phys.* **23** 149–57
- Fishkin J B, Coquoz O, Anderson E R, Brenner M and Tromberg B J 1997 Frequency-domain photon migration measurements of normal and malignant tissue optical properties in a human subject *Appl. Opt.* **36** 10–20
- Franceschini M A, Gratton E, Hueber D and Fantini S 1999 Near-infrared absorption and scattering spectra of tissues *in vivo Proc. SPIE* **3597** 526–31
- Franceschini M A, Moesta K T, Fantini S, Gaida G, Gratton E, Jess H, Seeber M, Schlag P M and Kashke M 1997 Frequency-domain techniques enhance optical mammography: initial clinical results *Proc. of Nat. Ac. of Sci* **94** 6468–73
- Gayen S K and Alfano R R 1999 Sensing lesions in tissues with light *Opt. Exp.* **4** 475–80 (webpage <http://epubs.osa.org/oearchive/source/9627.htm>)
- Gertig D M, Stillmann I E, Byrne C, Spiegelman D, Schnitt S J, Connolly J L, Colditz G A and Hunter D J 1999 Association of age and reproductive factors with benign breast tissue composition *Cancer Epidemiol. Biostat. Prev.* **8** 873–9
- Grosenick D, Wabnitz H, Rinneberg H H, Moesta K T and Schlag P M 1999 Development of a time-domain optical mammograph and first *in vivo* applications *Appl. Opt.* **38** 2927–43
- Gurfinkel M *et al* 2000 Pharmacokinetics of ICG and HPPH-car for the detection of normal and tumour tissue using fluorescence, near-infrared reflectance imaging: a case study *Photochem. Photobiol.* **72** 94–102
- Haskell R C, Svaasand L O, Tsay T, Feng T, McAddams M S and Tromberg B J 1994 Boundary Conditions for the diffusion equation in radiative transfer *J. Opt. Soc. Am. A* **11** 2727–41
- Hawrysz D J and Sevik-Muraca E 2000 Developments toward diagnostic breast cancer imaging using near-infrared optical measurements and fluorescent contrast agents *Neoplasia* **2** 388–417
- Hoogeraad J H, van der Mark M B, Colak S B, Hooft G W and van der Linden E S 1997 First results from the Philips optical mammoscope *Photon Propagation of tissues III* vol 3194, ed D A Benaron, B Chance and M Ferrari (SPIE) pp 184–90
- Kang K A, Chance B, Zhao S, Srinivasan S, Patterson E and Trouping R 1993 Breast tumour characterization using near-infra-red spectroscopy *Photon Migration and Imaging in Random Media and Tissues* vol 1888, ed R R Alfano and B Chance (Bellingham, WA: SPIE) pp 487–99
- Lee N A, Rusinek H, Weinreb J C, Chandra R, Singer R C and Newstead G M 1997 Fatty and fibroglandular tissue volumes in the breasts of women 20–83 years old: comparison of x-ray mammography and computer-assisted MR imaging *Am. J. Radiol.* **168** 501–06
- Li X D, Beauvoit B, White R, Nioka S, Chance B and Yodh A G 1985 Tumour localization using fluorescence of indocyanine green (ICG) in rat model *Proc. SPIE* **2389** 789
- Li X D, O'Leary M A, Boas D A, Chance B and Yodh A G 1996 Fluorescent diffuse photon-density waves in homogeneous and heterogeneous turbid media—analytic solutions and applications *Appl. Opt.* **35** 3746–58
- Mahmood U, Tung C H, Bogdanov A and Weissleder R 1999 Near-infrared optical imaging of protease activity for tumour detection *Radiology* **213** 866–70
- Martelli F, Contini D, Taddeucci A and Zaccanti G 1997 Photon migration through a turbid slab described by a model based on diffusion approximation: II. Comparison with Monte Carlo results *Appl. Opt.* **36** 4600–12
- McBride T O, Pogue B W, Gerety E D, Poplack S B, Osterberg U L and Paulsen K D 1999 Spectroscopic diffuse optical tomography for the quantitative assessment of hemoglobin concentration and oxygen saturation in breast tissue *Appl. Opt.* **38** 5480–90
- Mourant J R, Fuselier T, Boyer J, Johnson T M and Bigio I J 1997 Predictions and measurements of scattering and absorption over broad wavelength ranges in tissue phantoms *Appl. Opt.* **36** 949–57
- Nilsson A M, Stureson K C, Liu D L and Andersson-Engels S 1998 Changes in spectral shape of tissue optical properties in conjunction with laser-induced thermotherapy *Appl. Opt.* **37** 1256–67
- Nioka S, Miwa M, Orel S, Schnall M, Haida M, Zhao S and Chance B 1994 Optical imaging of human breast cancer *Adv. Exp. Med. Biol.* **361** 171–9
- Ntziachristos V and Chance B 2001 Probing physiology and molecular function using optical imaging: applications to breast cancer *Breast Cancer Res.* **3** 41–7
- Ntziachristos V, Ma X H and Chance B 1998 Time-correlated single photon counting imager for simultaneous magnetic resonance and near-infrared mammography *Rev. Sci. Instrum.* **69** 4221–33
- Ntziachristos V, Yodh A G, Schnall M and Chance B 1999 Comparison between intrinsic and extrinsic contrast for malignancy detection using NIR mammography *Proc. Optical Tomography and Spectroscopy of Tissue III* vol 3597, ed B Chance, R R Alfano and B J Tromberg (San Jose, CA: SPIE) pp 565–70

- Ntziachristos V, Yodh A G, Schnall M and Chance B 2000 Concurrent MRI and diffuse optical tomography of breast after indocyanine green enhancement *Proc. Nat. Acad. Sci. USA* **97** 2767–72
- O’Leary M A, Boas D A, Chance B and Yodh A G 1994 Reradiation and imaging of diffuse photon density waves using fluorescent inhomogeneities *J. Luminesc.* **60** 281–68
- Painchaud Y, Mailloux A, Harvey E, Verreault S, Frechette J, Gilbert C, Vernon M L and Beaudry P 1999 Multi-port time-domain laser mammography: results on solid phantom and volunteers *Int. Symp. Biomedical Optics* vol 3597 (Proc. SPIE) pp 548–55
- Peters V G, Wyman D R, Patterson M S and Frank G L 1990 Optical properties of normal and diseased human breast tissues in the visible and near infrared *Phys. Med. Biol.* **35** 1317–34
- Pogue B W, Poplack S D, McBride T O, Jiang S, Osterberg U L and Paulsen K D 2001a Near-infrared tomography: status of Dartmouth imaging studies and future directions (webpage <http://www.dartmouth.edu/~biolaser/>)
- Pogue B W, Poplack S P, McBride T O, Wells W A, Osterman K S, Osterberg U L and Paulsen K D 2001b Quantitative hemoglobin tomography with diffuse near infrared spectroscopy: pilot results in the breast *Radiology* **218** 261–6
- Prahl Scott 2001 Optical properties spectra (webpage <http://omlc.ogi.edu/spectra/index.html>)
- Sevick-Muraca E and Burch C L 1994 Origin of phosphorescence signals re-emitted from tissues *Opt. Lett.* **19** 1928–30
- Sickles E A 1984 Breast cancer detection with transillumination and mammography *Am. J. Roentgen.* **142** 841–4
- Suzuki K, Yamashita Y, Ohta K, Kaneko M, Yoshida M and Chance B 1996 Quantitative measurement of optical parameters in normal breasts using time-resolved spectroscopy: *in vivo* results of 30 Japanese women *J. Biomed. Opt.* **1** 330–4
- Thomsen S and Tatman D 1998 Physiological and pathological factors of human breast disease that can influence optical diagnosis *Adv. Opt. Biop. Opt. Mammography, Ann. N. Y. Acad. Sci.* **838** 171–93
- Tromberg B J, Coquoz O, Fishkin J, Pham T, Anderson E R, Butler J, Cahn M, Gross J D, Venugopalan V and Pham D 1997 Non-invasive measurements of breast tissue optical properties using frequency-domain photon migration *Philos. Trans. R. Soc. Lond. B: Biol. Sci.* **352** 661–8
- Troy T L, Page D L and Sevick-Muraca E 1996 Optical properties of normal and diseased breast tissue: prognosis for optical mammography *J. Biomed. Opt.* **1** 342–55
- Watmough D J 1982 Transillumination of breast tissues: factors governing optimal imaging of lesions *Radiology* **147** 89–92
- Weissleder R, Tung C H, Mahmood U and Bogdanov A 1999 *In vivo* imaging with protease-activated near-infrared fluorescent probes *Nat. Biotech.* **17** 375–8
- White D R, Woodard H Q and Hammond S M 1987 Average soft-tissue and bone models for use in radiation dosimetry *Br. J. Radiol.* **60** 907–13
- Woodard H Q and White D R 1986 The composition of body tissues *Br. J. Radiol.* **59** 1209–19
- Yang Y, Liu H, Li X and Chance B 1997 Low-cost frequency-domain photon migration instrument for tissue spectroscopy, oximetry and imaging *Opt. Eng.* **36** 1562–69